

Theory for measurements of penetration depth in magnetic superconductors by magnetic force microscopy and scanning SQUID microscopy

Shi-Zeng Lin and Lev N. Bulaevskii

Theoretical Division, Los Alamos National Laboratory, Los Alamos, New Mexico 87545, USA

(Received 6 June 2012; revised manuscript received 10 July 2012; published 23 July 2012)

The working principle of magnetic force microscopy and scanning SQUID microscopy is introducing a magnetic source near a superconductor and measuring the magnetic field distribution near the superconductor, from which one can obtain the penetration depth. We investigate the magnetic field distribution near the surface of a magnetic superconductor when a magnetic source is placed close to the superconductor, which can be used to extract both the penetration depth λ_L and magnetic susceptibility χ by magnetic force microscopy or scanning SQUID microscopy. When the magnetic moments are parallel to the surface, one extracts $\lambda_L/\sqrt{1-4\pi\chi}$. When the moments are perpendicular to the surface, one obtains λ_L . By changing the orientation of the crystal, one thus is able to extract both χ and λ_L .

DOI: [10.1103/PhysRevB.86.014518](https://doi.org/10.1103/PhysRevB.86.014518)

PACS number(s): 74.70.Dd, 74.25.Ha, 68.37.Rt, 85.25.Dq

I. INTRODUCTION

Superconductivity is well characterized by two length scales. The coherence length ξ describes the rigidity of the phase coherence and the penetration depth λ_L characterizes the response to electromagnetic fields. The penetration depth is directly connected to the superfluid density and the pairing symmetry, thus its measurement is crucial for the understanding of new discovered superconductors. The coherence length can be measured from the upper critical field H_{c2} for type-II superconductors. There are many well-developed methods to measure the penetration depth,¹ such as the magnetic force microscopy (MFM) and scanning SQUID microscopy (SSM), which are the main focus of this study.

In MFM and SSM, a magnetic source is placed near a superconductor.²⁻⁴ In MFM, the source magnetic field is generated by a small magnetic tip, which can be modeled as a point dipole. In SSM, the source field is generated by a current loop. Due to the exclusion of magnetic field by the superconductor, the magnetic field outside the superconductor is modified compared to that without the superconductor. The exclusion thus causes repulsion between the magnetic source and superconductor. In MFM, the resulting magnetic field distribution is measured by the force between the MFM tip and superconductor. In SSM, the magnetic field is measured by a SQUID. From the measured magnetic field, one can extract the penetration depth by fitting to theoretical expressions. For nonmagnetic superconductors, the magnetic field distribution was calculated in Refs. 5–9 for isotropic superconductors and in Ref. 10 for anisotropic superconductors.

Recently, there is growing interest to apply both MFM and SSM to magnetic superconductors, where magnetic ordering coexists with superconductivity.¹¹⁻¹³ When a magnetic field induced by a source is applied to the magnetic superconductors, it polarizes the magnetic moments near the surface of the superconductors, which gives additional contribution to the magnetic field outside the superconductors. The polarization is characterized by the magnetic susceptibility χ in the linear response approximation. For instance, in MFM, the polarization lowers the energy of the whole system, thus giving attraction contribution between the MFM tip and superconductor in addition to repulsion due to the screening

of magnetic field by superconductors. The magnetic field distribution outside the magnetic superconductor thus depends on χ and λ_L . It is still an open question as to what information can be extracted by MFM and SSM in the case of magnetic superconductors. Recently, Kirtley *et al.* studied the SSM response in isotropic paramagnetic superconductors.¹⁴ The effects of the isotropic paramagnet in this case are twofold. First, it reduces the penetration depth according to $\lambda_L\sqrt{1-4\pi\chi}$. Second, it changes the boundary condition. In isotropic paramagnetic superconductors, the magnetic field outside depends on $\lambda_L/\sqrt{1-4\pi\chi}$, and one can not extract both λ_L and χ from SSM measurements.

The magnetic superconductors usually have anisotropy in magnetic structure. The polarization depends on the orientation of the magnetic source with respect to the anisotropy of the magnetic structure. By changing the orientation of the crystal, it is possible to obtain both λ_L and χ .

In this work, we investigate the magnetic response in magnetic superconductors based on the London approach both in the Meissner state and the mixed state. For the magnetic moments parallel to the surface of the superconductor, the magnetic field outside the superconductor depends on $\lambda_L/\sqrt{1-4\pi\chi}$ when the separation between the magnetic source and superconductor is much larger than λ_L . For the moments perpendicular to the surface, it depends only on λ_L . By changing the orientation of the crystal, one thus can obtain both the bare penetration depth and the magnetic susceptibility.

II. MODEL

In this section, we derive the magnetic field distribution inside and outside the magnetic superconductor. A schematic view of the setup is shown in Fig. 1. To be specific, we consider the case with an easy-axis anisotropy in magnetic structure, which is most commonly encountered in magnetic superconductors.^{11,13} The penetration depth is assumed to be isotropic. We consider two cases with magnetic moment parallel to the surface [Fig. 1(a)] and perpendicular to the surface [Fig. 1(b)].

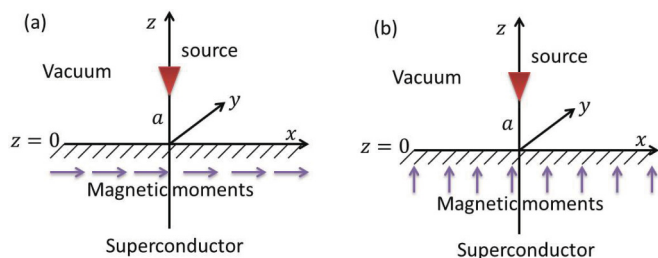


FIG. 1. (Color online) Schematic view of a magnetic source placed on top of a magnetic superconductor. The magnetic subsystem has easy-axis anisotropy. The easy axis is parallel to the surface in (a) or perpendicular to the surface in (b).

The magnetic field outside the superconductor is given by

$$\nabla \times (\mathbf{B} - 4\pi \mathbf{M}_s) = 0, \quad (1)$$

where \mathbf{M}_s is the magnetization in the source. Using $\nabla \cdot \mathbf{B} = 0$, we can rewrite Eq. (1) as

$$\nabla^2 \mathbf{B} = -4\pi \nabla \times \nabla \times \mathbf{M}_s. \quad (2)$$

Inside the superconductor, we use the London approximation, which is valid when the penetration length is much larger than the coherence length as realized in most magnetic superconductors:^{11,15–17}

$$\lambda_L^2 \nabla \times \nabla \times (\mathbf{B} - 4\pi \mathbf{M}) + \mathbf{B} = \Phi_0 \delta(x) \delta(y) \hat{z}, \quad (3)$$

where \hat{z} is the unit vector along the z axis and $\Phi_0 = hc/(2e)$ is the flux quantum. We assume the vortex density is small when the applied magnetic field is much smaller than H_{c2} , and we only consider a single vortex at $(x, y) = (0, 0)$.

The magnetic field outside and inside the superconductor is connected through the boundary conditions at the interface $z = 0$. The normal component of \mathbf{B} is continuous at the interface

$$B_z(z = 0^-) = B_z(z = 0^+). \quad (4)$$

As the induced surface supercurrent is finite at the interface, from the Maxwell equations we have the boundary condition for the tangential component $B_{x,y}$:

$$\begin{pmatrix} B_x(z = 0^-) \\ B_y(z = 0^-) \end{pmatrix} - 4\pi \begin{pmatrix} M_x(z = 0^-) \\ M_y(z = 0^-) \end{pmatrix} = \begin{pmatrix} B_x(z = 0^+) \\ B_y(z = 0^+) \end{pmatrix}. \quad (5)$$

The general solution to Eq. (2) can be written as $\mathbf{B} = \mathbf{B}_1 + \mathbf{B}_2$, where \mathbf{B}_1 and \mathbf{B}_2 are solutions of Eq. (2) with \mathbf{M}_s and without \mathbf{M}_s , respectively. $\mathbf{B}_2(\mathbf{r})$ can be written as

$$\mathbf{B}_2(\mathbf{r}) = \frac{1}{(2\pi)^{3/2}} \int dk_x dk_y \mathbf{B}_2(k) \exp[i\mathbf{k}_{2d} \cdot \mathbf{r}_{2d} - k_{2d}z], \quad (6)$$

where $\mathbf{k}_{2d} = (k_x, k_y)$ and $\mathbf{r}_{2d} = (x, y)$. To solve the London equation (3), we need to know the magnetic structure of the magnetic superconductor. In the following sections, we treat the cases with magnetic moments perpendicular and

parallel to the interface separately using the linear response approximation for the magnetization.

A. Magnetic moments parallel to the interface

We assume the easy axis is along the x direction. The magnetization can be written as $M_x = \chi B_x$, which is valid when $M_x \ll M_0$ with M_0 being the saturation magnetization. The solution to Eq. (3) can be written as $\mathbf{B} = \mathbf{B}_3 + \mathbf{B}_4$ with \mathbf{B}_3 accounting for the magnetic fields induced by the vortex and \mathbf{B}_4 being the solution to Eq. (3) in the absence of vortices. Since the vortex is along the z axis, we have $B_{3,x} = B_{3,y} = 0$ and

$$B_{3,z}(k_x, k_y) = \frac{\Phi_0}{2\pi(\mathbf{k}_{2d}^2 \lambda_L^2 + 1)}. \quad (7)$$

\mathbf{B}_4 in the Fourier space is given by

$$(\mathbf{k}^2 \lambda_L^2 + 1) B_{4,x} - 4\pi \lambda_L^2 (k_y^2 + k_z^2) \chi B_{4,x} = 0, \quad (8)$$

$$(\mathbf{k}^2 \lambda_L^2 + 1) \begin{pmatrix} B_{4,y} \\ B_{4,z} \end{pmatrix} + 4\pi \lambda_L^2 k_x \begin{pmatrix} k_y \\ k_z \end{pmatrix} \chi B_{4,x} = 0. \quad (9)$$

From Eq. (8), we obtain

$$k_z^2 = \frac{4\pi \chi k_y^2 - \lambda_L^{-2} - \mathbf{k}_{2d}^2}{1 - 4\pi \chi}. \quad (10)$$

From Eq. (9), we obtain

$$B_{4,y} = -\frac{k_x k_y}{k_y^2 + k_z^2} B_{4,x} \quad \text{and} \quad B_{4,z} = -\frac{k_x k_z}{k_y^2 + k_z^2} B_{4,x}. \quad (11)$$

Using the boundary conditions (4) and (5), we have for $\mathbf{B}(\mathbf{k}_{2d}, z = 0)$

$$-\frac{1}{\sqrt{2\pi}} \frac{k_x k_z}{k_y^2 + k_z^2} B_{4,x} + \frac{\Phi_0}{2\pi(\mathbf{k}_{2d}^2 \lambda_L^2 + 1)} = B_{1,z} + B_{2,z}, \quad (12)$$

$$-\frac{1}{\sqrt{2\pi}} \frac{k_x k_y}{k_y^2 + k_z^2} B_{4,x} = B_{1,y} + B_{2,y}, \quad (13)$$

$$\frac{1 - 4\pi \chi}{\sqrt{2\pi}} B_{4,x} = B_{1,x} + B_{2,x}. \quad (14)$$

Using $\nabla \cdot \mathbf{B}_2 = 0$, we can derive the field $B_{4,x}$ from Eqs. (12)–(14). Substituting the results back into Eq. (12), we have the magnetic fields outside the superconductor $B_{2,z} = B_{s,z} + B_{v,z}$, with the contribution from the magnetic source

$$\begin{aligned} B_{s,z}(\mathbf{k}_{2d}, z = 0) \\ = -\alpha \left[\left(k_{2d} + \frac{1}{\alpha} \right) B_{1,z} - i k_x B_{1,x} - i k_y B_{1,y} \right], \end{aligned} \quad (15)$$

and the contribution from the vortex

$$B_{v,z}(\mathbf{k}_{2d}, z = 0) = (\alpha k_{2d} + 1) \frac{\Phi_0}{2\pi(\mathbf{k}_{2d}^2 \lambda_L^2 + 1)}, \quad (16)$$

with

$$\alpha(k_x, k_y) = -k_z [k_z k_{2d} + i k_z^2 - i 4\pi \chi (k_y^2 + k_z^2)]^{-1}. \quad (17)$$

The magnetic field outside the superconductor then is given by

$$B_{2,z}(\mathbf{r}) = \int \frac{d^2 k_{2d}}{2\pi} B_{2,z}(\mathbf{k}_{2d}, z = 0) \exp(-k_{2d}z + i\mathbf{k}_{2d} \cdot \mathbf{r}_{2d}). \quad (18)$$

Since the magnetic moments couple directly to the magnetic induction \mathbf{B} , we use the definition that $\chi = M_x/B_x$. In literatures (for examples see Refs. 14–16), another definition $\chi' = M_x/H_x$ was used, where $\mathbf{H} = \mathbf{B} - 4\pi\mathbf{M}$ is the external field “seen” by the magnetic moments. The relation between χ and χ' is $\chi' = \chi/(1 - 4\pi\chi)$. If χ' is introduced, one should replace $\sqrt{1 - 4\pi\chi}$ in the results of this work by $1/\sqrt{1 + 4\pi\chi'}$. Please note that the magnetic susceptibility $\chi = M_x/B_x$ is smaller than $1/(4\pi)$, i.e., $\chi < 1/(4\pi)$. The magnetic fluctuations $\langle M_x M_x \rangle \sim \chi/(1 - 4\pi\chi)$ diverge when $\chi \rightarrow 1/(4\pi)$, which indicates that the magnetic system becomes unstable.¹⁸

B. Magnetic moment perpendicular to the interface

The calculations in this case are in parallel to those in the previous section. Here, we skip the detailed calculations and only present the final results. The results can be obtained from Eqs. (15) and (16) by replacing α and k_z with

$$\alpha(k_x, k_y) = -(k_{2d} + ik_z)^{-1}, \quad (19)$$

$$k_z^2 = -\lambda_L^{-2} - \mathbf{k}_{2d}^2(1 - 4\pi\chi). \quad (20)$$

III. APPLYING TO MFM AND SSM

We have derived the general expressions for the magnetic field distribution $B_{2,z}$ outside the superconductor in response to the source field $B_{1,z}$. In the following section, we consider the cases of MFM and SSM, respectively. For MFM, the magnetic source is modeled as a point dipole or monopole, and we then calculate the force between the MFM tip and superconductors. For SSM, the source is modeled as a current loop and we calculate $B_{2,z}$. In both cases, the source magnetic field is extremely weak, thus no additional vortex is induced by the source.

A. Magnetic force microscopy

In MFM, the force between the magnetic tip and the superconductor is measured as function of the distance between them.¹⁹ To calculate the force, one needs to know the magnetic field distribution inside the tip. Theoretical modeling of the tip is challenging since the magnetic field distribution and shape of the tip are generally unknown. In most treatments, one assumes a single cylindrical magnetic domain with spatially uniformly distributed moments perpendicular to the sample surface.^{20,21} If the length of the cylinder is much larger than its radius, one can approximate the tip as a magnetic monopole. Otherwise, the tip behaviors as a dipole. First, we model the MFM tip by a point dipole along the z direction:

$$\mathbf{M}_s = m_0 \delta(x) \delta(y) \delta(z - a) \hat{\mathbf{z}}, \quad (21)$$

where a is the separation between the MFM tip and the superconductor. The approximation of the tip by a point dipole is valid when the size of the tip is much smaller than a . The typical size of the tip is tens of nanometers. For $a \gg \lambda_L$, it was shown that the shape of the MFM tip will not affect the

results substantially.⁵ \mathbf{B}_1 then can be expressed as

$$B_{1,z}(\mathbf{k}_{2d}, z = 0) = m_0 \exp(-ak_{2d})k_{2d}, \quad (22)$$

$$\begin{pmatrix} B_{1,x}(\mathbf{k}_{2d}, z = 0) \\ B_{1,y}(\mathbf{k}_{2d}, z = 0) \end{pmatrix} = im_0 \exp(-ak_{2d}) \begin{pmatrix} k_x \\ k_y \end{pmatrix}. \quad (23)$$

The interaction between the tip and magnetic field is

$$\begin{aligned} U(a) &= - \int d^3r M_z(B_{1,z} + B_{2,z}) \\ &= -m_0[B_{1,z}(0,0,a) + B_{2,z}(0,0,a)]. \end{aligned} \quad (24)$$

The force then is given by $F = -\partial_a U(a) = F_s + F_v$ with the contribution from the source

$$F_s = \frac{m_0^2}{\pi} \int (2\alpha k_{2d} + 1) \exp(-2ak_{2d}) \mathbf{k}_{2d}^2 d^2k_{2d}, \quad (25)$$

and the contribution from the vortex

$$F_v = \frac{m_0 \Phi_0}{(2\pi)^2} \int \frac{\alpha \mathbf{k}_{2d}^2 + k_{2d}}{\mathbf{k}_{2d}^2 \lambda_L^2 + 1} \exp(-ak_{2d}) d^2k_{2d}. \quad (26)$$

Analytical expression for the force can be obtained when $a \gg \lambda_L$. In this case, only small \mathbf{k}_{2d} contributes to the integration. For the magnetic moments parallel to the interface, we obtain

$$F_{\parallel,s} = \frac{3m_0^2}{4\lambda_L^4} \left(\frac{\lambda_L^4}{a^4} - 4 \frac{\lambda_L^5}{a^5 \sqrt{1 - 4\pi\chi}} \right), \quad (27)$$

$$F_{\parallel,v} = \frac{m_0 \Phi_0}{\lambda_L^3 \pi} \left(\frac{3\lambda_L^4}{a^4 \sqrt{1 - 4\pi\chi}} - \frac{\lambda_L^3}{a^3} \right). \quad (28)$$

For the magnetic moments perpendicular to the interface, we have

$$F_{\perp,s} = \frac{3m_0^2}{4\lambda_L^4} \left(\frac{\lambda_L^4}{a^4} - 4 \frac{\lambda_L^5}{a^5} \right), \quad (29)$$

$$F_{\perp,v} = \frac{m_0 \Phi_0}{\lambda_L^3 \pi} \left(\frac{3\lambda_L^4}{a^4} - \frac{\lambda_L^3}{a^3} \right). \quad (30)$$

The exclusion of the magnetic flux by the superconductor gives rise to repulsion between the tip and superconductor, which is described by the first term in Eqs. (27) and (29). The force does not depend on the direction of the point dipole. For a magnetic superconductor, the polarization of magnetic moment reduces energy and causes attraction, as described by the second term in Eqs. (27) and (29). When the separation a reduces, the attraction may be even larger than the repulsion, as shown by direct numerical integration of Eqs. (25) in Figs. 2 and 3. The attraction increases with χ .

The interaction between the vortex and tip depends on the direction of the dipole and it is attractive at large separation $a \gg \lambda_L$ when they are parallel. To visualize a vortex, one scans the tip in experiments, and the force depends on the vortex position relative to the tip. The position dependence of the force can be readily evaluated by replacing $\Phi_0 \leftarrow \Phi_0 \exp[i(k_x x_v + k_y y_v)]$. Here, $r_v = (x_v, y_v)$ is the coordinate of the vortex core. For $a \gg \lambda_L$, the vortex-position-dependent force is

$$F(r_v = 0) - F(r_v) = -\frac{3m_0 \Phi_0}{\pi^2} \frac{\lambda_L^2}{a^5} r_v^2. \quad (31)$$

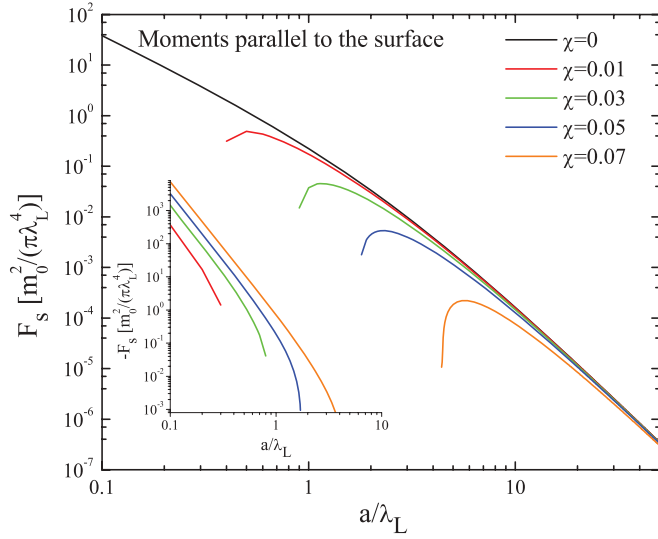


FIG. 2. (Color online) Force between a magnetic tip and magnetic superconductor in the absence of vortices obtained by numerical integration of Eq. (25) when the magnetic moments are parallel to the surface. For small a/λ_L , the interaction becomes attractive for nonzero χ as shown in the inset. At large $a/\lambda_L \gg 1$, the curves are described by Eq. (27).

To extract the penetration depth in experiments, one measures the force as a function of a in the absence of vortex. One then obtains the penetration depth by fitting to theoretical expressions, such as Eq. (25). In the magnetic superconductors, the force depends on the orientation of the magnetic moments with respect to the surface. For the magnetic moments parallel to the surface, one extracts an effective penetration depth $\lambda_L/\sqrt{1-4\pi\chi}$ [see Eq. (27)]. For the moments perpendicular to the surface, the bare penetration depth λ_L is extracted [see Eq. (29)]. By measuring the force in two different orientations, one can extract both χ and λ_L .

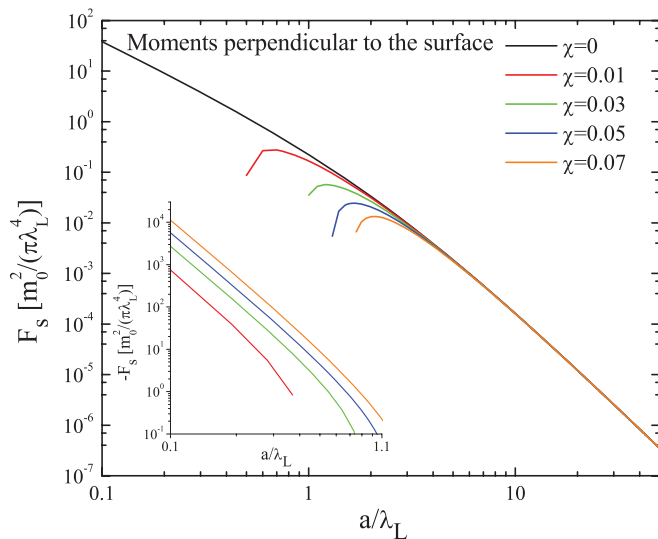


FIG. 3. (Color online) The same as Fig. 2 but for the magnetic moments perpendicular to the surface. Results are obtained by numerical integration of Eq. (25).

We proceed to model the magnetic tip as a monopole and calculate the interaction force. The magnetic field outside the superconductor is given by

$$\nabla \cdot \mathbf{B} = 4\pi n_0 \delta(x)\delta(y)\delta(z-a), \quad \nabla \times \mathbf{B} = 0. \quad (32)$$

Here, n_0 is a magnetic charge. The magnetic field distribution outside $B_{2,z}$ can still be calculated with Eqs. (15) and (18) with α and k_z given by Eqs. (10), (17), (19), and (20) depending on the orientation of the magnetic moments inside the superconductor. \mathbf{B}_1 in this case is given by

$$B_{1,z}(\mathbf{k}_{2d}, z=0) = -n_0 \exp(-ak_{2d}), \quad (33)$$

$$\begin{pmatrix} B_{1,x}(\mathbf{k}_{2d}, z=0) \\ B_{1,y}(\mathbf{k}_{2d}, z=0) \end{pmatrix} = -in_0 \frac{\exp(-ak_{2d})}{k_{2d}} \begin{pmatrix} k_x \\ k_y \end{pmatrix}. \quad (34)$$

The z -component force is given by $F = n_0 B_{2,z}(0,0,a)$. When the magnetic moments are parallel to the surface, we obtain the force due to the source $F_{\parallel,s}$ and the force due to vortex $F_{\parallel,v}$ in the limit $a \gg \lambda_L$:

$$F_{\parallel,s} = \frac{n_0^2}{\lambda_L^2} \left(\frac{\lambda_L^2}{4a^2} - \frac{\lambda_L^3}{2a^3 \sqrt{1-4\pi\chi}} \right), \quad (35)$$

$$F_{\parallel,v} = \frac{n_0 \Phi_0}{2\pi \lambda_L^2} \left(\frac{\lambda_L^2}{a^2} - \frac{4\lambda_L^3}{a^3 \sqrt{1-4\pi\chi}} \right). \quad (36)$$

For the magnetic moments perpendicular to the surface, we have

$$F_{\perp,s} = \frac{n_0^2}{\lambda_L^2} \left(\frac{\lambda_L^2}{4a^2} - \frac{\lambda_L^3}{2a^3} \right), \quad (37)$$

$$F_{\perp,v} = \frac{n_0 \Phi_0}{2\pi \lambda_L^2} \left(\frac{\lambda_L^2}{a^2} - \frac{4\lambda_L^3}{a^3} \right). \quad (38)$$

In the limits $\chi \rightarrow 0$ and $\lambda_L \rightarrow 0$, one can model the superconductor as a perfect magnetic conductor and the magnetic field outside the superconductor can be obtained with the image method. If one models the MFM tip as a magnetic dipole, the repulsion between the image dipole and tip is $3m_0^2/(4a^4)$. If the tip is treated as a monopole, the repulsion force is $n_0^2/(4a^2)$. Both Eqs. (27) and (35) reproduce the limiting results.

B. Scanning SQUID microscopy

In SSM, one applies external magnetic field through a field coil and then measures the magnetic field above the superconductor through a pickup loop.^{4,14} We model the field coil by a loop with current I and radius r_0 . Please note that when $a \gg r_0$, the magnetic field induced by the current loop is reduced to the point dipole discussed in the previous section. The source magnetic field due to the current loop is then given by $\mathbf{B}_1 = \nabla \varphi$ with the magnetic potential¹⁰

$$\varphi(r) = \int d^2 k_{2d} \varphi(\mathbf{k}_{2d}) \exp[i\mathbf{k}_{2d} \cdot \mathbf{r}_{2d} + k_{2d} z], \quad (39)$$

$$\varphi(\mathbf{k}_{2d}) = \frac{r_0 I}{ck_{2d}} \exp(-k_{2d} a) J_1(k_{2d} r_0). \quad (40)$$

In this case, the magnetic field outside the superconductor due to the source field is

$$B_{s,z}(\mathbf{k}_{2d}, z=0) = -\alpha \left(2k_{2d} + \frac{1}{\alpha} \right) \frac{2\pi I a}{c} \times J_1(k_{2d} r_0) \exp(-k_{2d} a) \quad (41)$$

and the vortex contribution is the same as Eq. (16). Here, α depends on the orientation of the magnetic moments. For the moments parallel to the surface, α is given by Eq. (17) and for the moments perpendicular to the surface it is given by Eq. (19). When the magnetic moments are parallel to the surface, the magnetic field at the center of the pickup loop is given by (for $a \gg \lambda_L$)

$$B_{s,z} = \frac{\pi I r_0^2}{4ca^3} \left(-1 + \frac{3\lambda_L}{a\sqrt{1-4\pi\chi}} \right), \quad (42)$$

$$B_{v,z} = \frac{\Phi_0}{2\pi a^2} \left(1 - \frac{2\lambda_L}{a\sqrt{1-4\pi\chi}} \right). \quad (43)$$

For the moments perpendicular to the surface, the results are the same as those in Eqs. (42) and (43), but without the factor $\sqrt{1-4\pi\chi}$, similar to the case of MFM.

In the case of a magnetic superconductor with isotropic magnetic structure as studied in Ref. 14, the magnetic field outside the superconductor is given by Eqs. (42) and (43).

The extracted penetration depth from SSM measurements is $\lambda_L/\sqrt{1-4\pi\chi}$, which is larger than the bare λ_L . This is different from the effective penetration depth in magnetic superconductors $\lambda_L\sqrt{1-4\pi\chi}$, which is smaller than the bare λ_L .

IV. CONCLUSION

We have calculated the magnetic fields outside a magnetic superconductor when a magnetic source is placed on top of the superconductor. For the magnetic moments parallel to the surface, the resulting magnetic field distribution depends on an effective penetration depth $\lambda_L/\sqrt{1-4\pi\chi}$ when the distance between the magnetic source and superconductor is much larger than λ_L , while for the moments perpendicular to the surface, it depends on λ_L . The results in this work can be used to measure both the susceptibility χ and the penetration depth λ_L in magnetic superconductor by the magnetic force microscopy or scanning SQUID microscopy. This can be achieved by changing the orientation of the crystal.

ACKNOWLEDGMENTS

The authors thank J. Kim and M. M. Graf for helpful discussions. This work was supported by the US Department of Energy, Office of Basic Energy Sciences, Division of Materials Sciences and Engineering.

-
- ¹R. Prozorov and R. W. Giannetta, *Supercond. Sci. Technol.* **19**, R41 (2006).
²J. R. Kirtley, C. C. Tsuei, M. Rupp, J. Z. Sun, L. S. Yu-Jahnes, A. Gupta, M. B. Ketchen, K. A. Moler, and M. Bhushan, *Phys. Rev. Lett.* **76**, 1336 (1996).
³J. R. Kirtley, C. C. Tsuei, K. A. Moler, V. G. Kogan, J. R. Clem, and A. J. Turberfield, *Appl. Phys. Lett.* **74**, 4011 (1999).
⁴J. R. Kirtley, *Rep. Prog. Phys.* **73**, 126501 (2010).
⁵J. H. Xu, J. H. Miller, and C. S. Ting, *Phys. Rev. B* **51**, 424 (1995).
⁶M. W. Coffey, *Phys. Rev. B* **52**, R9851 (1995).
⁷M. W. Coffey, *Phys. Rev. B* **57**, 11648 (1998).
⁸M. W. Coffey, *Phys. Rev. Lett.* **83**, 1648 (1999).
⁹A. Badía, *Phys. Rev. B* **63**, 094502 (2001).
¹⁰V. G. Kogan, *Phys. Rev. B* **68**, 104511 (2003).
¹¹L. N. Bulaevskii, A. I. Buzdin, M. L. Kubic, and S. V. Panjukov, *Adv. Phys.* **34**, 175 (1985).

- ¹²A. I. Buzdin, *Rev. Mod. Phys.* **77**, 935 (2005).
¹³L. C. Gupta, *Adv. Phys.* **55**, 691 (2006).
¹⁴J. R. Kirtley, B. Kalisky, J. A. Bert, C. Bell, M. Kim, Y. Hikita, H. Y. Hwang, J. H. Ngai, Y. Segal, F. J. Walker, C. H. Ahn, and K. A. Moler, *Phys. Rev. B* **85**, 224518 (2012).
¹⁵M. Tachiki, H. Matsumoto, and H. Umezawa, *Phys. Rev. B* **20**, 1915 (1979).
¹⁶K. E. Gray, *Phys. Rev. B* **27**, 4157 (1983).
¹⁷A. I. Buzdin and L. N. Bulaevskii, *Usp. Fiz. Nauk* **149**, 45 (1986) [*Sov. Phys. Usp.* **29**, 412 (1986)].
¹⁸E. I. Blount and C. M. Varma, *Phys. Rev. Lett.* **42**, 1079 (1979).
¹⁹L. Luan, O. M. Auslaender, T. M. Lippman, C. W. Hicks, B. Kalisky, J. Chu, J. G. Analytis, I. R. Fisher, J. R. Kirtley, and K. A. Moler, *Phys. Rev. B* **81**, 100501 (2010).
²⁰H. J. Hug, Th. Jung, H.-J. Günterodt, and H. Thomas, *Phys. C (Amsterdam)* **175**, 357 (1991).
²¹S. J. Bending, *Adv. Phys.* **48**, 449 (1999).